

Evaluation of hot hardness and creep of a 350 grade commercial maraging steel

U.K. VISWANATHAN, T.R.G. KUTTY, R. KESWANI, C. GANGULY
Radiometallurgy Division, Bhabha Atomic Research Centre, Bombay 400 085, India

The hardening response and the indentation creep of a 350 grade commercial maraging steel were evaluated using a hot hardness tester. The hardness versus temperature plot exhibited three distinct regions. Hardness response was noted between 500–800 K. The unusually high values of activation energy and stress exponent obtained during the creep experiment could be rationalized by a novel concept of introducing a back stress term in the indentation creep relation. The corrected value of the activation energy was found to be reasonably in agreement with the activation energy for diffusion of Ni in iron. Results are supplemented with microstructural observation.

1. Introduction

The need for an alloy with ultra-high strength combined with adequate toughness led to the development of a class of low-carbon high-nickel steels, known as 18Ni maraging steels [1, 2]. By and large, these steels are based on the Fe–18%Ni binary alloy with additions of various alloying elements such as cobalt, molybdenum, titanium and aluminium for precipitation hardening. The grades of these steels are denoted by numbers such as 200, 250, 300 or 350, the number specifying the level of the yield strength in ksi that can be obtained in the steel with appropriate heat treatments.

Though considerable work has been carried out in the past in generating data on the mechanical properties of lower grades, only limited information is available in the open literature on the mechanical properties of 350 grade of maraging steel [3]. Data available on the mechanical properties of maraging steel at elevated temperature are very few and most of the studies on the low grades were confined to tensile properties or stress-rupture studies up to 811 K [4–6]. Specialized applications of the steel occasionally demand short-time exposures at unusually high temperatures and it is desirable to have data on the creep behaviour of the material during such service conditions.

Indentation creep of polycrystalline materials is a well known phenomenon. The evaluation of creep parameters by using an indentation technique has become a very popular method for assessing metals, intermetallics, ceramics and superalloys since rapid and reliable information can be generated by this technique [7–14]. In this work the indentation creep properties of a 350 grade commercial maraging steel are evaluated by carrying out microhardness measurements at elevated temperatures.

2. Method, material and experimental procedure

The indentation creep process can be defined as the time dependent penetration of a hard indenter into

the material under constant load and temperature. The indenter maintains its load over a period of time under well controlled conditions and the changes in the size of the indentation are monitored during the experiment. The indentation creep model developed by Li et al. [15] assumes that if the indentation has a diameter d , there is a hemispherical core of material of radius a below the indenter, which is under hydrostatic pressure, equal to the indentation pressure. From the boundary of this core, plastic flow spreads into the surrounding material and the plastic strain gradually diminishes until it equals the elastic strain in the hinterland at some radius c at the elastic–plastic boundary. Creep deformation cannot occur in the hydrostatic core below the indenter due to the absence of any shear stress in the zone. However, in the elastic–plastic zone, the stress field is deviatoric, thereby exerting forces on the defects present in the material causing the material to creep.

Mulhelan and Tabor [16] have related hardness (H), dwell time (t) and temperature (T in K) by the following relation:

$$H^{-n} = A \exp(-Q/RT)t \quad (1)$$

where n is the stress exponent. A is the material constant and Q is the activation energy.

Atkin and co-workers [17] have demonstrated that the dynamic microindentation hardness for a variety of materials at temperatures above $0.5 T_m$, where T_m is the melting point (in K), closely parallels the viscous creep behaviour. During the microindentation creep, the plastic zone continuously increases with load time and the application of the transient creep equation is more appropriate than the viscous creep relation. Consequently, it has been postulated [17] that the kinematics of creep can be analysed by using a transient creep equation of the form:

$$H^{-n/3} - H_0^{-n/3} = A_2 \exp(-Q/3RT)(t^{1/3} - t_0^{1/3}) \quad (2)$$

where H is the hardness at time t and H_0 is the hardness at time t_0 , the time required during the

TABLE I Chemical composition of the 350 grade maraging steel in (wt %)

| C | Mn | Co | Ni | Mo | Ti | Al | S | P | Fe |
|--------|-------|-------|-------|------|------|------|--------|-------|------|
| 0.0046 | 0.021 | 12.32 | 18.39 | 3.99 | 1.63 | 0.12 | 0.0028 | 0.005 | bal. |

indentation to attain full hardness, which is normally found to be 0.5 s and A_2 is a constant.

Equation 2 predicts a linear plot of $(H^{-n/3} - H_0^{-n/3})$ versus $(t^{1/3} - t_0^{1/3})$ with a slope of unity. The activation energy for the rate controlling process of creep can thus be calculated by knowing the interval on the abscissa between two lines at temperatures T_1 and T_2 by the following relation:

$$Q = \frac{3R[C_1 - C_2]}{[1/T_1 - 1/T_2]} \quad (3)$$

where $(C_1 - C_2)$ is the interval on the abscissa

The maraging steel used in this study was a forged bar, 70 mm in diameter, in the double solution-annealed condition. The solution annealing consisted of a first anneal at 950°C for 2 h, followed by air cooling and a second anneal at 820°C for 3.5 h, followed by air cooling. The chemical composition of the alloy is given in Table I. Samples of 6 mm diameter and 7 mm length were machined from the raw stock.

The hot hardness experiments were carried out on metallographically polished samples by using a Nikon Model QM Hot Hardness Tester fitted with a diamond micro Vickers indenter. Both the sample and indenter can be heated and controlled independently to an accuracy of ± 1 K. The experiments were conducted in vacuum (0.1 Pa) using a load of 10 N. The length of the diagonal was measured at $500\times$ with an accuracy of $\pm 0.5 \mu\text{m}$. The hardness was estimated using the relation:

$$H = 1854.4 P/d^2 \quad (4)$$

where P is the load in grams and d is the average length of the diagonal in micrometres.

In order to study the hardening response of the steel, hardness was measured on a solutionized sample heated from room temperature to 1173 K at every 100 K intervals, using a dwell time of 5 s. Another set of samples were aged at 783 K for 3 h using the hot hardness furnace and cooled to room temperature. Creep measurements were carried out on these aged samples at temperatures between 723–1073 K for dwell times of 1, 5, 10, 30, 100 and 300 s. At each temperature and time at least four indentations were made and the average value is reported.

Thin foils for transmission electron microscopy (TEM) were prepared by a window technique, using an electrolyte containing 60% methanol, 34% *n*-butanol and 6% perchloric acid. The temperature of the electrolyte was kept below 243 K. Microstructural examination was carried out in a Jeol 2000FX electron microscope.

3. Results and discussion

While heating, a number of solid state reactions occur in maraging steel. The reaction products are very fine

and are beyond the resolution limit of optical microscopy. Therefore, unlike in the case of metals and ceramics, *in situ* examination of the microstructure during the creep experiment is not possible. However, using transmission electron microscopy, the microstructural evolution in this alloy during isothermal heat treatments has been studied in detail and the results are reported elsewhere [18]. The microstructure in the as-solution treated condition essentially consisted of fine lath martensites with a high density of dislocations and was devoid of any precipitates. Fig. 1a shows a typical microstructure of the alloy in the as-solution treated condition. Strengthening is achieved in this alloy by the precipitation of intermetallic phases of the type $\text{Ni}_3(\text{Ti},\text{Mo})$ and $\text{Fe}_2(\text{Mo})$ [18]. The dark field micrograph of the alloy aged at 783 K for 3 h, taken using a $\text{Ni}_3(\text{Ti},\text{Mo})$ reflection is shown in Fig. 1b. The micrograph shows the uniform distribution of the fine needle-shaped precipitates of $\text{Ni}_3(\text{Ti},\text{Mo})$ in the matrix. Ageing at higher temperatures led to the dissolution of the precipitates and the simultaneous nucleation of austenite in regions which are rich in nickel [1]. The room temperature microstructure of the alloy heat treated at these temperatures shows the presence of austenite as well as precipitates. Fig. 1c shows the room temperature microstructure of the alloy overaged at 848 K for 8 h, in which the retained austenite is present as shown by the arrow.

The hardness versus temperature plot of the alloy is shown in Fig. 2. Three distinct regions could be identified from Fig. 1, namely, (i) an initial decrease up to 473 K; (ii) a rapid increase up to 800 K followed by (iii) a continuous decrease. The decrease in hardness up to 473 K is typically due to the softening of the alloy. It is noted that beyond 473 K the hardening response of the alloy was so fast and that maximum hardness was attained at 800 K. The absence of an incubation period and the rapid onset of hardening are consistent with earlier findings [18, 19]. The decrease in hardness above 800 K is due to the coarsening of the intermetallic precipitates and the formation of the austenite phase.

The creep behaviour of the alloy aged at 783 K for 3 h is studied at different temperatures. The results are depicted in Fig. 3 as plots between $\ln(H)$ and $\ln(t)$, where t is the dwell time (in seconds) of indentation. The stress exponent n is calculated from the slope of the straight line. The material showed good resistance against creep at 773 and 803 K, as can be inferred from the near horizontal shape of the plots. However, at higher temperatures, the material exhibited an increasing tendency to creep.

In order to evaluate the kinematics of the creep by using Equations 2 and 3 the data are replotted between $(H^{-n/3} - H_0^{-n/3})$ and $(t^{1/3} - t_0^{1/3})$ on a logarithmic scale and presented in Fig. 4. The values of

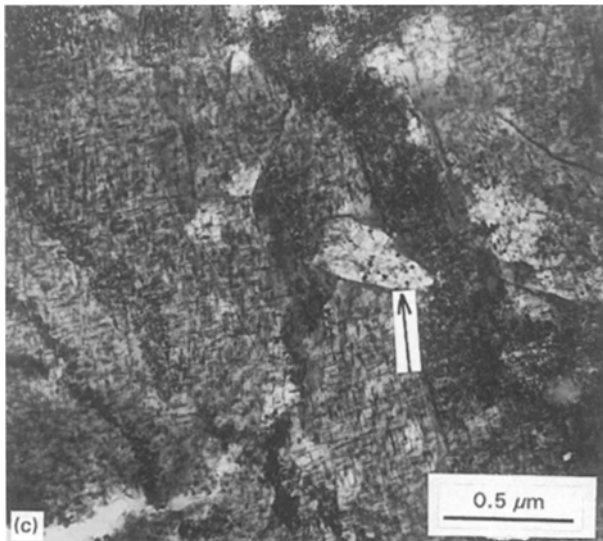
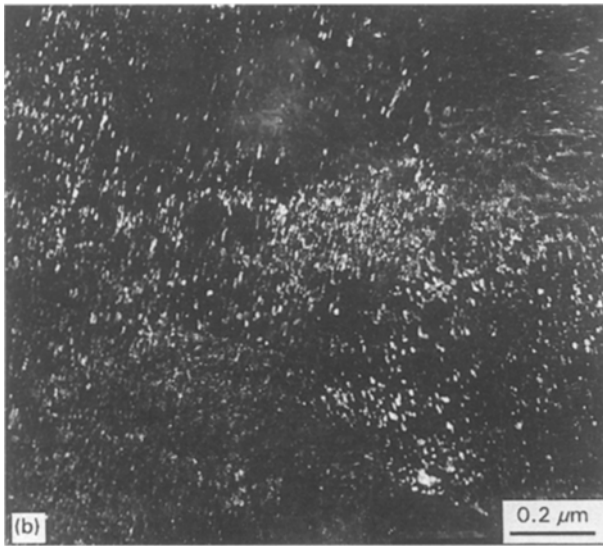
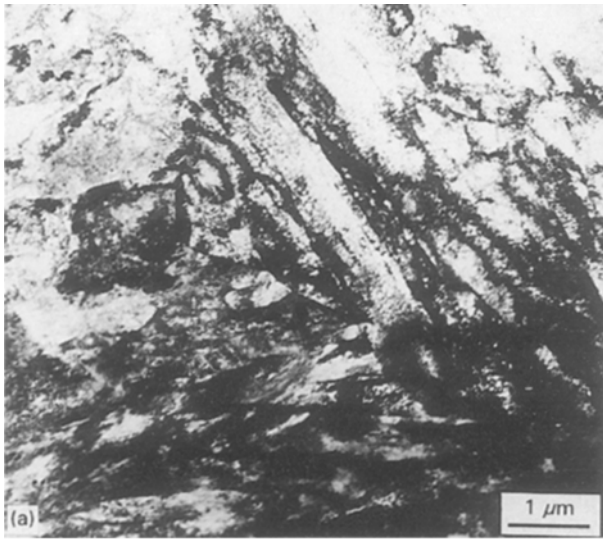


Figure 1 (a) Microstructure of the alloy in as-solution treated condition. (b) Darkfield micrograph of the alloy aged at 783 K for 3 h, showing the uniform distribution of $\text{Ni}_3(\text{Ti}, \text{Mo})$ precipitates. (c) Microstructure of the alloy overaged at 848 K for 8 h, showing the presence of austenite along with intermetallic particles.

n and Q determined from the plots are given in Table II.

The results show that the estimated values of n and Q are unusually high and also that they are temperature dependent. In many dispersion and precipitation

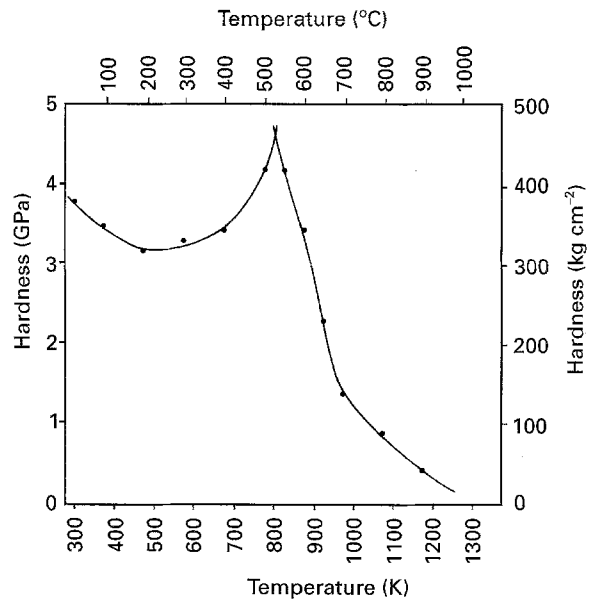


Figure 2 Hardness versus temperature plot of the alloy.

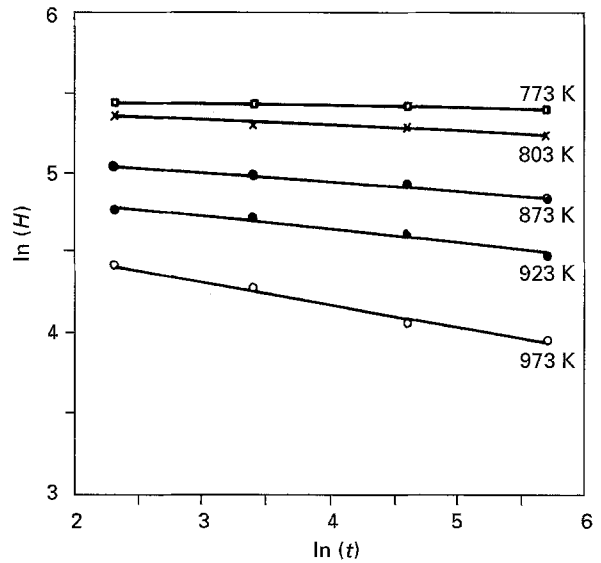


Figure 3 Plots between $\ln(H)$ and $\ln(t)$.

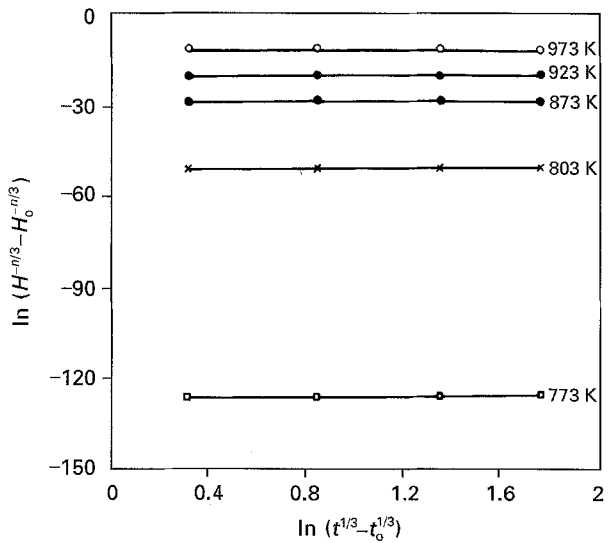


Figure 4 Plots between $\ln(H^{-n/3} - H_0^{-n/3})$ and $\ln(t^{1/3} - t_0^{1/3})$.

TABLE II The apparent values of stress exponent and activation energy

| Temperature (K) | n | Q (kJ mol ⁻¹) |
|-----------------|------|-----------------------------|
| 773 | 69.2 | 38945 |
| 803 | 28.0 | |
| 873 | 16.4 | 3411 |
| 923 | 11.9 | 3800 |
| 973 | 7.2 | |

strengthened alloys, the experimentally estimated values of n and Q are abnormally high [20, 21]. Purushotham and Tien [22] have reported an n value of ~ 35 for an oxide dispersion strengthened (ODS) superalloy. Similarly, Lund and Nix [23] have obtained n values of the order of 75 for a dispersion strengthened system. Similarly, in the case of many particle strengthened systems, activation energies of 4 to 5 times the self diffusion values have been reported [23].

These high values of n and Q are not considered as the true reflection of the thermally activated process but are attributed to the presence of the back stress [12]. The back stress or the resisting stress (σ_b), is due to the resistance offered by the strengthening particles and other obstacles to the motion of dislocations. It has also been reported [12] that this unusually high value of n could be reduced if the creep rate is described in terms of an effective stress (σ_e) which is the applied stress minus the back stress.

For evaluating the magnitude of the back stress as a function of temperature and also to rationalize the apparent high activation energy obtained for creep, the experimental data were analysed in terms of the modified equation for dispersion and precipitation strengthened alloys [24] :

$$\begin{aligned} & (H - \sigma_b)^{-n'/3} - (H_0 - \sigma_b)^{-n'/3} \\ & = A_3 \exp(-Q'/3RT)(t^{1/3} - t_0^{1/3}) \end{aligned} \quad (5)$$

where n' and Q' are the corrected stress exponent and activation energy, respectively, and σ_b is the back stress.

In this treatment, n was assigned a fixed value of 4.5, which is found to be a physically reasonable value for this type of alloy [22]. The estimated back stress and the corrected activation energy values at different temperatures are given in Table III. It can be noted from Table III that the magnitude of back stress is reduced as the temperature is increased and the corrected activation energy values approached a narrow band over the whole range of temperature.

The estimated values of back stress and the apparent activation energy need to be examined in the context of the microstructural instability of the alloy at the experimental temperatures. By using a dilatometric technique it was established [19] that at a heating rate of 10 K min⁻¹, the precipitation of intermetallic phases in this alloy started at 783 K.

TABLE III Back stress and the corrected activation energy for creep of maraging steel

| Temperature (K) | Back stress, σ_b (kJ mm ⁻²) | Corrected activation energy Q' (kJ mol ⁻¹) |
|-----------------|--|--|
| 773 | 205.6 | 548 |
| 803 | 155.0 | |
| 873 | 93.0 | 405 |
| 923 | 57.0 | 467 |
| 973 | 20.0 | |

Further heating led to the coarsening of the precipitates and to their subsequent dissolution. On continuous heating, nucleation of austenite is thought to initiate around the regions which are rich in nickel. The austenite reversion start (A_s) and the austenite reversion finish (A_f) temperatures for this alloy at this heating rate were reported to be 946 and 1057 K, respectively [19].

The gradual change in the back stress with temperature could be considered to be due to the instability of the alloy microstructure at high temperatures. With the onset of austenite reversion, dissolution of the precipitates could be considered as the dominant process. Beyond the A_s temperature diffusion of the austenite stabilizer Ni into the austenite grain is the rate controlling process. The corrected activation energy for the creep behaviour, therefore, could not be rationalized in terms of a specific mechanism since a number of simultaneous mechanisms control the formation of austenite. The dissolution of the intermetallic precipitates is governed by the bond energy of the precipitates (in this case Ni₃(Ti, Mo) and Fe₂Mo). The bond energy of Ni₃Mo is reported to be between 418–836 kJ mol⁻¹ [25]. Activation energy for diffusion of Ni, Ti or Mo either into ferrite or into austenite is reported to be lower than the corrected activation energy values obtained in this study. Hence, the values could be considered only as a weighed average of the two interfering mechanisms namely, the dissolution of the precipitates and the diffusion of the species of the precipitates into the newly formed austenite.

Before concluding it may be pointed out that the indentation technique used for evaluating the high temperature creep properties must not be considered as a substitution for the conventional tensile creep test used for material types such as maraging steel, mainly due to the instability of the microstructure during the prolonged exposure at elevated temperature. Results presented in this paper can be applied only to short-term or accidental exposures to high temperature and the extrapolation of the results to higher temperatures or to extended periods of exposure should be carried out with caution.

4. Conclusions

The hardness creep test provides a simple and non-destructive method of investigating mechanical

properties of maraging steel and provides information on the creep properties. The following conclusions are made in this study:

(i) Hardness versus temperature plot of 350 grade maraging steel has three distinct regions as compared to two for conventional alloys. The hardness at intermediate temperatures increases sharply with temperature and shows a peak at 800 K.

(ii) The stress exponent and activation energy calculated from the $\log H$ versus $\log t$ plot in the temperature range of 773 K–973 K exhibited unusually high values. The apparent activation energy at low temperature was found to decrease with increasing temperature.

(iii) A novel concept of incorporating a back stress term in the indentation creep relation was adopted for maraging steel and the corrected activation energy was found to be reasonably in agreement with the activation energy for diffusion of Ni in Fe.

(iv) The back stress was found to decrease with increasing temperature and was almost negligible at 923 K.

Acknowledgement

The authors thankfully acknowledge the experimental support received from Dr G. K. Dey in carrying out the TEM examinations.

References

1. S. FLOREEN, *Metall. Rev.* **13** (1968) 115.
2. R. F. DECKER, *Adv. Mater. Process Inc., Metal Prog.* **6** (1988) 45.
3. H. J. RACK, *Mater. Sci. Eng.* **34** (1978) 263.
4. S. FLOREEN and R. F. DECKER, *ASM Trans. Q.* **56** (1963) 403–11.
5. A. F. HOENIE, AFML-TR-65-197, North American Aviation, (July 1965).
6. G. MARTIN, *Mater Design Eng.* (December 1964) 56.
7. J. H. WESTBROOK, *Trans. Amer. Soc. Metals* **45** (1953) 221.
8. J. LARSEN-BADSE, AEC Report ORNL-TM-1771 (1967).
9. T. G. NIEH and J. WADSWORTH, *Scripta Metall.* **23** (1989) 1261.
10. G. M. CARTER, J. L. HENSHALL and R. M. COOPER, *Commun. Amer. Ceram. Soc.* **71** (1988) C-27.
11. KUMASHIRO, A. ITOH, T. KINOSHITA and M. SOBAYIMA, *J. Mater. Sci.* **12** (1977) 595.
12. G. E. VIGNOUL, J. K. TIEN and J. M. SANCHEZ, *Mater. Sci. Eng. A* **170** (1993) 177.
13. A. B. RODRIGUEZ, E. P. BARTH and J. K. TIEN, in *Material Research Society Symposium Proceedings*, Vol. 213, Nov. 27–30, 1990, Boston, USA (Materials Research Society, Pittsburgh, PA, 1992) 539.
14. G. A. GEACH, *Int. Metall. Rev.* **19** (1974) 255.
15. W. B. LI, J. M. HENSHALL, R. M. HOOPER and K. E. EASTERLING, *Acta Metall.* **39** (1991) 3099.
16. T. O. MULHELAN and D. TABOR, *J. Inst. Metals* **89** (1960–61) 7.
17. A. G. ATKINS, A. SILVERIO and D. TABOR, *ibid.* **94** (1966) 369.
18. U. K. VISWANATHAN, G. K. DEY and M. K. ASUNDI, *Metall. Trans.* **24A** (1993) 2429.
19. U. K. VISWANATHAN, T. R. G. KUTTY and C. GANGULY, *ibid.* **24A** (1993) 2653.
20. T. E. HOWSON, J. E. STULGSA, and J. K. TIEN, *ibid.* **11A** (1980) 1599.
21. J. P. PETROVIC and L. J. EBERT, *ibid.* **4A** (1973) 1301.
22. S. PURUSHOTHAM and J. K. TIEN, *Acta Metall.* **26** (1978) 159.
23. R. W. LUND and W. D. NIX, *ibid.* **24A** (1976) 469.
24. G. E. VIGNOUL, J. M. SANCHEZ and J. K. TIEN, *Mater. Res. Symp. Proc.* **213** (1991) 739.
25. N. JAYARAMAN, PhD thesis, Indian Institute of Science, Bangalore, India (1978).

Received 1 June 1994
and accepted 9 November 1995